AIRBORNE TESTING OF THE DSS: TEST RESULTS AND ANALYSIS

Mohamed M.R. Mostafa

Applanix Corporation, 85 Leek Cr., Richmond Hill, Ontario, Canada L4B 3B3 – mmostafa@applanix.com

SS3

KEY WORDS: Airborne Mapping, Aerial Triangulation, Direct Georeferencing, GPS/INS, Digital, Camera, Calibration

ABSTRACT:

In this paper, the Digital Sensor System (DSS) test results and analysis are presented. The DSS is a fully integrated fully digital ruggedized system for airborne image acquisition, georeferencing, and map production. The DSS consists of a 4K x 4K digital camera, a GPS-aided INS direct georeferencing system, and a flight management system. The DSS software suite interfaces seamlessly with commercial off-the-shelf photogrammetric software to allow for fast topographic and ortho map production. The DSS currently uses a CCD chip with a 9 µm pixel size which allows digital image acquisition with a Ground Sample Distance that ranges from 0.05 m to 1.0 m using its 35 mm and 55 mm lenses. The embedded POS AV direct georeferencing system provides the exterior orientation parameters in both real-time and post-mission modes. The DSS is used primarily to generate high-resolution color and color infrared digital orthophotos, orthomosaics, and topographic maps, which can be used for many different mapping, GIS and remote sensing applications.

1. INTRODUCTION

In the mid 1990s, digital camera technology started to attract several Photogrammetrists. Several efforts have been exerted to deploy the CCD-based digital camera technology into the airborne mapping environment. Some of these efforts focused on using a digital camera in a stand-alone mode (c.f., King et al, 1994; Mills et al, 1996). More efforts focused on using digital cameras as a component of an integrated system (c.f., Mostafa et al, 1997; Toth and Grejner-Brzezinska, 1998) where the System integration concept was initially proposed by Schwarz et al (1993) and Schwarz, 1995.

In this paper, The Digital Sensor System (DSS) is introduced as a dedicated product that is designed for the airborne mapping industry based on the aforementioned scientific research and several years of experience of using such systems. The performance of the DSS in s number of mapping projects is introduced in some details

Figure 1: The DSS

The DSS, shown in Figure 1, is a fully digital integrated ruggedized system for airborne image acquisition, georeferencing, and map production. The DSS hardware consists of a 4K x 4K digital camera, a GPS-aided INS direct georeferencing system, and a flight management system. The DSS comes with a suite of data processing software package for GPS-aided inertial data processing and analysis, data calibration and quality control, and mission planning, calibration and quality control. The DSS software suite interfaces seamlessly with commercial off-the-shelf photogrammetric software to allow for fast topographic and ortho map production. The DSS currently uses a CCD chip with a 9 µm pixel size which allows digital image acquisition with a Ground Sample Distance that ranges from 0.05 m to 1.0 m (platform dependent) using its 35 mm and 55 mm lenses. The embedded POS AV direct georeferencing system provides the exterior orientation parameters in both real-time and post-mission modes. The DSS is used primarily to generate high-resolution color and color infrared digital orthophotos, orthomosaics, and topographic maps, which can be used for many different mapping, GIS and remote sensing applications. For details, see Mostafa, 2003.

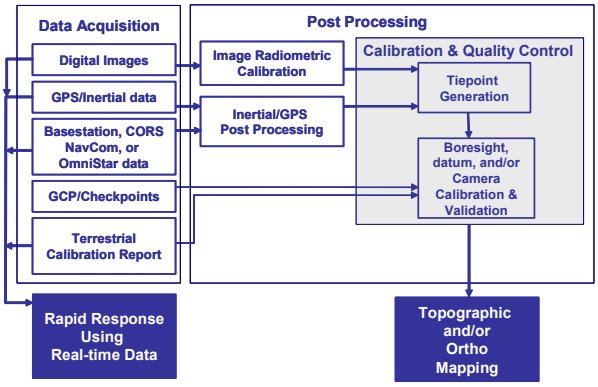

Figure 2: The DSS Data Flow

The DSS collects digital images and navigation data. The navigation (GPS/inertial) data is processed in real time based on either the GPS C/A code GPS data, or Satellite RTK data such as Navcom or OmniStar as data shown in Figure 2. In this case, the real-time navigation data together with the digital images are processed once the aeroplane is landed in a matter of a few hours for rapid response applications.

For precision applications, however, the navigation data is either processed using a single dedicated GPS basestation or multiple base stations such as the CORS (c.f., Snay, 2000). In post-mission, the precise navigation data together with the digital images go through calibration and quality control for precision mapping purposes, where a number of accurate and well distributed tie points are generated in fully or semi-automatic mode, which are then used to perform a calibration and quality control procedure to refine the boresight, camera, and datum calibration parameters, as shown in Figure 2

2. TERRESTRIAL CALIBRATION RESULTS AND ANALYSIS

The geometric accuracy of the mapping products produced using the DSS data depends on the resolution and the accuracy of each single component of the entire system and the accuracy of the calibration parameters of the system components and the system as a whole. This section is dedicated to present the results of the terrestrial calibration of the DSS system.

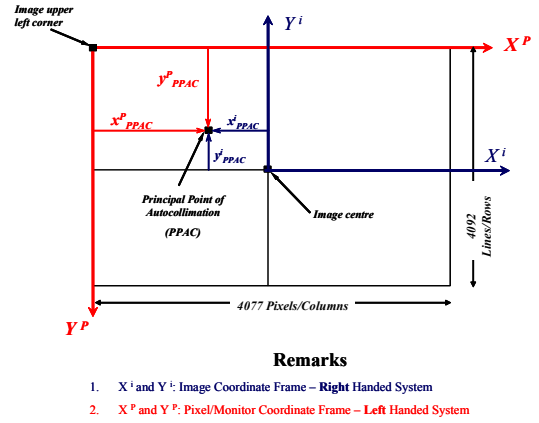

Figure 3: The DSS Image Coordinate System

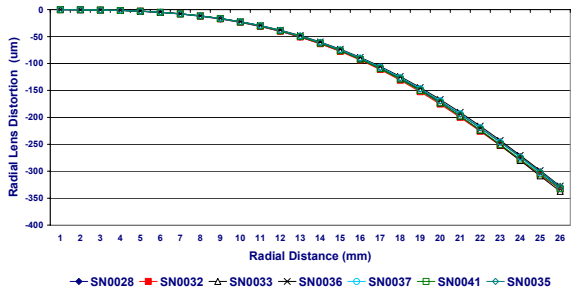

Figure 4: Radial Lens Distortion Profile for Different DSS Systems – 55 mm lenses

The terrestrial calibration is done using traditional digital camera calibration techniques (c.f., Beyer, 1992, Fraser, 1997, Lichti and Chapman, 1997) using a target field consisting of over 160 well surveyed targets with a sub-millimetre surveying precision surveyed by a Total Station. This target field is imaged by the DSS system in close-range from different surveyed locations and with different orientation angles to allow for precise calibration of the focal length, principal point offsets, and lens distortion, as well as an initial value of the boresight parameters. For details, see Mostafa, 2003 for the DSS and Mostafa and Schwarz 2000 and Mostafa and Schwarz, 2001 for a detailed description of the overall system calibration.

As shown in Figure 3, the position of the principal point of autocollimation is computed in the image coordinate frame and the boresight angles rotating that frame into the IMU frame are also computed during the DSS terrestrial calibration. Although the radial lens distortion of the lenses is normally large, as shown in Figure 4, it is calibrated in the terrestrial mode and compensated for in the photogrammetric reconstruction of image rays during the map compilation mode.

Figure 5 shows the repeatability of the radial lens distortion profiles using different lenses (shown in Figure 4) when compared to the first lens profile. It is noticeable that the difference between the radial distortions of totally different lenses is well within one pixel (9 um). This seems to indicate that the lenses used by the DSS possess almost similar radial distortion character and implies that these lenses can be swapped in the field which will result in a positional error contribution of no more than one pixel at the image edge, without recalibrating the system. However, this is not recommended to be done in the normal practice since there is no guarantee that this conclusion is consistent and it is always best to calibrate the lens in the terrestrial mode where the geometry of the calibration data is a lot more controlled than that of the airborne environment.

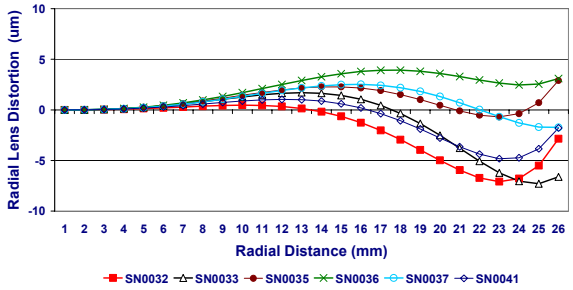

Figure 5: Repeatability of Radial Lens Distortion for Different DSS Systems

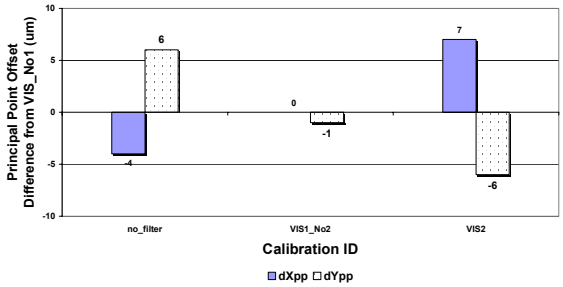

Figure 6: Principal Point Difference Using Different Filters

Figure 6 shows the difference in the calibrated principal point offsets where a lens filter is removed (no_filter) and then placed back on the lens (VIS1_No2) and totally replaced by a new filter (VIS2). When the lens filter is placed back on the lens and the system is re-calibrated, the difference of the principal point offsets is no more than one micron. On the other hand, when no filter is used or a totally new filter is used, the difference in the calibrated principal point offsets is well within one pixel, which is easily calibrate during the airborne quality control procedure discussed later. This indicates that the DSS user can replace lens filters without the need for recalibrating the DSS system in the case of the Rapid Response applications. It is recommended, however, to calibrate each lens together with its filter in the terrestrial mode for precision mapping applications.

Generally speaking, the terrestrially calibrated parameters can be directly used for map production. This approach is efficient and provides adequate accuracy for rapid response applications. However, for precision mapping applications, another more precise alternative is used; where a part of the airborne survey data is used to refine the calibrated parameters. This approach is called Calibration and Quality Control. This approach has been experimented earlier and showed viable (c.f., Mostafa and Schwarz, 2001) where a number of well distributed tie points are automatically or semi/automatically generated and used together with the GPS/INS exterior orientation parameters and the terrestrially calibrated parameters to compute a refined system calibration parameters under the flight conditions at hand.

3. THE DSS TEST FLIGHTS

The DSS is frequently being test flown for performance evaluation purposes. The results of a number of DSS test flights are presented in this paper. This section is dedicated to briefly introduce the flight configuration of each of these flights.

In December, 2002, the DSS was flown over a test field in Lakeland, Florida, USA. This flight will be referred to as Lakeland Dec02. The Lakeland test field has a total of 37 ground control points (GCPs). The flight altitude is about 2000 m which when coupled with the 55 mm focal length of the lens in use, results in a Ground Sample Distance (GSD) of about 0.3 m. Six strips of images were flown where a total of 65 images were collected. Two more flights were flown over the same test field in January 2004 and March 2004, respectively. These two flights will be referred to as Lakeland Jan04 and Lakeland Mar04, respectively.

Flight ID	Flight Altitude AGL (m)	GSD (m)	#Strips/ #Photos	# Check Points
Lakeland Dec02	1800	0.3	6/65	37
Lakeland Jan04	1200 & 1800	0.3 & 0.5	6/30	30
Lakeland Mar04	1200 & 1800	0.2 & 0.3	5/30	32
NASA Stennis	1800	0.3	12/242	9
Japan Feb03	1200 & 1800	0.2 & 0.3	5/41	60
Ajax 03	1200	0.2	9/165	46
PASCO Toyonaka	300	0.05	6/150	16

Table 1: Configuration Parameters of Different DSS Flights

NASA Stennis Space Centre has independently evaluated a test flight data set especially acquired for that purpose. The same data set has been evaluated independently at Applanix and the results are presented here. In February 2003, a set of data was collected in Japan where a total of 41 images over 5 strips were collected over a test field which has about 60 GCPs. In August, 2003 a test flight was flown over Southern Ontario, Canada, where a part of this test flight data was flown over Ajax, Ontario and will be referred to as Ajax 03. Note that the test flights discussed so far have been flown to attain a GSD of about 0.2 m, 0.3 m, and 0.5 m. PASCO Corporation flew a rather high resolution test flight over Toyonaka City in Japan, where the flight altitude is 300 m which resulted in a GSD of about 0.05 m. This flight will be referred to as PASCO Toyonaka flight. Table 1 lists a summary of the configuration parameters of the aforementioned flights. An example of the flight trajectories of these flights is shown in Figure 7, where the Southern Ontario flight trajectory is plotted and the Ajax part of this flight is highlighted near the upper right corner of Figure 7.

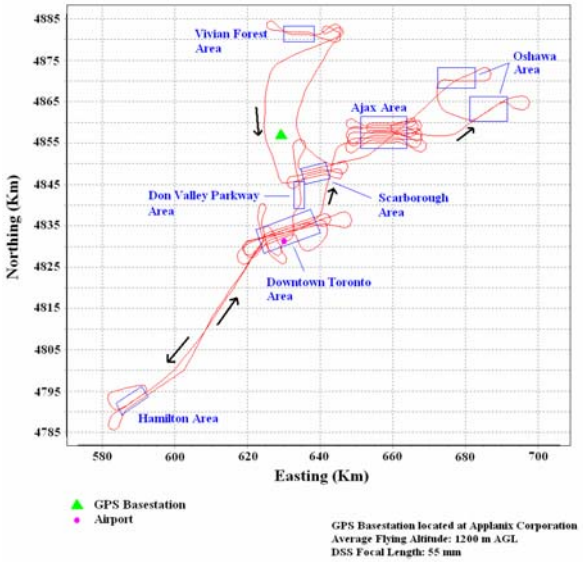

Figure 7: Southern Ontario Test Flight Trajectory

4. TEST FLIGHT RESULTS AND ANALYSIS

As mentioned above, the DSS test flights were flown for performance evaluation purposes. The most important parameter in the performance evaluation of a survey system is the absolute accuracy of the system when examined against a known reference. Therefore, the efficient way of analyzing the performance of the DSS is to compare the DSS-derived checkpoint coordinates to those surveyed independently by land surveying techniques. The statistics of checkpoint residuals simply depict the final absolute accuracy of the checkpoints. Moreover, the minimum and maximum values of the residuals show the error bounds for individual points. In addition, the mean value of the residuals show whether or not there is remaining biases in the system.

In the following discussion, the results from a number of the DSS test flights are presented using the aforementioned checkpoint residuals as an evaluation criterion. Some of the data results have been previously presented in some detail in Mostafa (2003), Tachibana et al (1004) and Ip et al (2004). The presentation herein is, therefore, rather concise and focused on the repeatability of the DSS system performance in the different test flights discussed in Section 3.

Note that all the results presented here are after the DSS data has gone through the airborne calibration and quality control procedure shown in Figure 2.

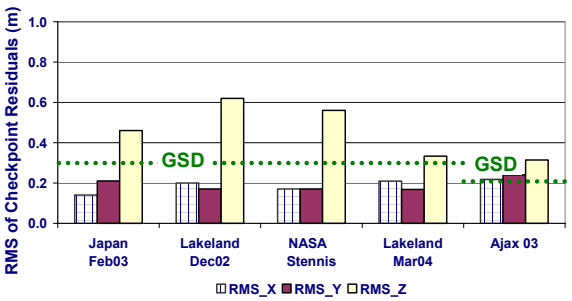

Figure 8: Statistics of Checkpoint Residuals for Different DSS Test Flights – 55 mm Lens

Each of the test flight data sets discussed here is processed similarly by following the data flow represented in Figure 2, where the DSS image data is radiometrically balanced while the POS AV GPS-aided inertial data is processed. Then the image data, the exterior orientation parameters, and the system calibration parameters are run through an airborne calibration and quality control procedure. Then the data is used to produce ground coordinates of the available checkpoints.

The resulting coordinates are then compared to those computed independently using land surveying techniques. The resulting checkpoint residuals are listed in Table 2, while the RMS values are shown in Figure 8 and Figure 9.

Flight	Statistic	y-parallax (um)	dX (m)	dY (m)	dZ (m)
Lakeland Dec02	Min	0.2	-0.76	-0.51	-1.89
	Max	13.1	0.53	1.14	1.68
	Mean	3.1	-0.08	-0.06	-0.09
	RMS	**4.9**	**0.29**	**0.29**	**0.77**
NASA Stennis	Min	1.7	-0.39	-0.49	-1.47
	Max	12.3	0.71	0.39	1.15
	Mean	4.9	0.02	0.00	-0.13
	RMS	**5.2**	**0.19**	**0.17**	**0.44**
Japan Feb03	Min	0.0	-0.33	-0.33	-0.77
	Max	7.8	0.04	0.23	0.77
	Mean	2.8	-0.09	-0.08	-0.11
	RMS	**3.7**	**0.14**	**0.21**	**0.56**
Ajax03 0.2m GSD	Min	0.0	-0.39	-0.55	-0.82
	Max	22.7	0.56	0.44	0.67
	Mean	4.6	-0.04	-0.01	-0.12
	RMS	**5.7**	**0.22**	**0.24**	**0.31**
Lakeland Mar04 0.3 m GSD	Min	3.0	-0.36	-0.24	-0.58
	Max	11.9	0.16	0.28	0.71
	Mean	5.5	-0.13	-0.05	0.09
	RMS	**6.0**	**0.21**	**0.17**	**0.33**
Lakeland Mar04 0.2 m GSD	Min	3.0	-0.29	-0.14	-0.34
	Max	9.0	-0.04	0.42	0.21
	Mean	5.0	-0.14	0.05	-0.10
	RMS	**5.1**	**0.17**	**0.22**	**0.22**

Table 2: Statistics of Checkpoint Residuals for Different DSS Test Flights - 55 mm lens

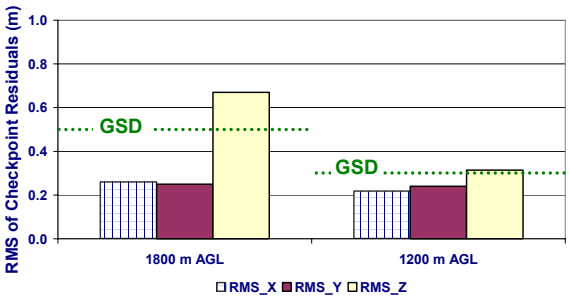

Figure 9: Statistics of Checkpoint Residuals for Lakeland Jan04 Test Flight - 35 mm Lens - Two Flight Altitudes

Note that in Table 2, the first three flights have a common GSD of 0.3 m, while the Ajax 03 flight and the Lakeland Mar04 flights have a 0.2 m GSD which explains the rather higher accuracy, especially in the elevation. The first column in the statistics in Table 2 shows the remaining y-parallax, which is well within one pixel, which indicates the great capability of the DSS data for stereo mapping. Figure 8 shows the RMS of checkpoint residuals for the test flights flown with a 55 mm lens. Note the different GSD imposed on the Ajax03 flight in Figure 8. Figure 9 shows the RMS of checkpoint residuals for the Lakeland Jan04 flight flown using a 35 mm lens for the two different flight altitudes. It is clear from Figure 8 and Figure 9 that the accuracy of the checkpoints is within ½ to ¾ of the GSD in the horizontal components and around 1 to 2 times of the GSD in the elevation.

5. INTEGRATED SENSOR ORIENTATION USING THE DSS FOR LARGE SCALE MAPPING

To evaluate the performance of the DSS for large scale mapping applications, the DSS has been flown by PASCO Corporation over Toyonaka city in Japan in February, 2003. For details, see Tachibana et al (2004). The DSS was mounted onboard an AS350B helicopter shown in Figure 10 which was flown at about 300 m flight altitude, resulting in 0.05 m GSD. At this rather large scale, the GPS data would be the dominant source of error as far as the geometric accuracy is concerned. Therefore, the DSS data has been processed using the Integrated Sensor Orientation method (ISO) where an aerotriangulation scheme is used to process all the data to come up with the best fit. For details, see Heipke et al (2001). The results of the test flight are described in some detail in Tachibana et al (2004).

Figure 10: AS350B Helicopter Used for PASCO Toyonaka 0.05m GSD Test Flight in Japan

Statistic	dX (m)	dY (m)	dXY (m)	dZ (m)	Remarks
RMS	0.04	0.07	0.08	0.15	No GCPs
Max	0.11	-0.14	0.15	-0.36	16 Checkpoints
RMS	0.04	0.07	0.08	0.13	1 GCP Used
Max	0.10	-0.14	0.14	0.30	15 Checkpoints
RMS	0.06	0.05	0.07	0.17	4 GCPs
Max	-0.09	-0.09	0.10	-0.38	12 Checkpoints

Table 3: Statistics of Check Point Residuals Using the Integrated Sensor Orientation Concept - PASCO Toyonaka 0.05m GSD Test Flight (after Tachibana et al, 2004)

A number of tests have been done to evaluate the performance of the DSS using the ISO concept. The results of using the ISO in different configurations are listed in Table 3, where the statistics of the checkpoint residuals are shown for three different cases: using no GCPs, using one GCP, and using 4 GCPs, respectively. Note that the results are consistent among the three mentioned configurations. Also, note that using no GCPs still means that the ISO concept has been used. Tachibana et al (2004) concluded that the DSS performance when flown a 0.05 m GSD and using the ISO concept results in an accuracy that meets the Japanese mapping accuracy standards for 1:500 scale mapping.

6. AUTOMATED ORTHOMOSAIC PRODUCTION USING THE DSS DATA

To evaluate the map production capabilities of the DSS data, one of the data sets of the Southern Ontario flights has been used to produce a Digital Elevation Model (DEM) and an orthophoto mosaic. The data has been airborne calibrated and quality controlled using the same procedure discussed earlier. Then the DSS images together with the exterior orientation parameters were used in ERDAS to automatically generate a DEM with no manual interaction or editing. The resulting DEM has been used together with the georeferenced images to produce an orthophoto mosaic, shown in Figure 11.

All the data flow was done automatically on ERDAS and without using ground control. The location of checkpoints were measured on the resulting orthophoto mosaic and compared to the land-surveyed ones. The statistics of the checkpoint residuals are listed in Table 4. Note that the final absolute orthophoto mosaic accuracy is about 1.5 of the GSD. For a detailed discussion, see Ip et al (2004).

Type	Overall Area			
	dX		dY	
	(m)	GSD	(m)	GSD
Min	-0.09	-0.5	-0.28	-1.4
Max	0.67	3.4	0.59	3.0
Mean	0.02	0.1	0.06	0.3
RMS	0.29	1.5	0.30	1.5
# check points	40			

Table 4: Orthomosaic Checkpoint Residuals

7. SUMMARY AND OUTLOOK

In this paper, the test results of a number of test flights flown by the DSS are presented. The results show consistent performance of the DSS between different test flights. After performing the airborne calibration and quality control, the accuracy of the checkpoint residuals was consistently about ½ to ¾ the GSD in the horizontal components while about twice as much in the elevation. Evaluating the orthophoto mosaic produced using the DSS data showed that the orthomosaic checkpoint residuals are accurate to 1.5 times the GSD in both X and Y components.

Figure 11: Automated Orthophoto Mosaic produced using the Ajax03 DSS Test Flight

8. ACKNOWLEDGEMENTS

Z/I Imaging Corporation provided the ISAT software which has been used in the automated tie point generation and EO analysis used in this research. Leica Geosystems provided the ERDAS Imagine software which has been used for the DEM generation and orthophoto production used to process the DEM and Orthomosaic of the Ajax flight. Aircraft and Crew were provided by The Airborne Sensing Corporation, Toronto, Canada. BAE Systems provided Socet Set for internal research and analysis. NOAA collected the ground control points in

Lakeland, Florida. Mr. Kikuo Tachibana of PASCO Corporation, Japan, processed and analyzed the PASCO Toyonaka City 5-cm resolution DSS Flights and allowed for publishing the results herein. Thanks to Rosalind Bobbit for processing the multiple basestation solution for Lakeland 2003 and NASA Stennis flights, Alan Ip for processing the Ajax DEM and orthomosaic on ERDAS Imagine, Greg Lipa for managing data acquisition, and Ernest Yap for terrestrial DSS calibration data acquisition.

9. REFERENCES

Beyer, H.A., 1992. Geometric and Radiometric Analysis of a CCD-Camera Based photogrammetric Close-Range System, Ph.D. Thesis, Institut für Geodäsie und Photogrammetrie, ETH-Hönggerberg, CH-8093 Zürich, Mitteilungen Nr. 51.

Braun, J., 2003. Aspects on True-Orthophoto Production. Proceedings of the 49th Photogrammetric Week, Stuttgart, Germany, September 1-5.

Grejner-Brezezinska, D.A., 2001. Direct Sensor Orientation in Airborne and Land-based Mapping Application. Report No. 461, Geodetic GeoInformation Science, Department of Civil and Environmental Engineering and Geodetic Science, The Ohio State University.

Fraser, C.S., 1997. Digital Camera Self Calibration, ISPRS Journal of Photogrammetry & Remote Sensing, 52(1997): 149-159.

Heipke, C, Jacobsen, K, Wegmann, H, Andersen, O and Nilsen, B., 2000. Integrated Sensor Orientation-An OEEPE Test. IAPRS, Vol. XXXIII, Amsterdam, 2000.

Ip, A.W.L., M.M.R. Mostafa, and N. El-Sheimy, 2004. Fast Orthophoto Production Using The Digital Sensor System. Proceedings of the 7th Annual International Conference - Map India 2004, New Delhi, India, January 28-30.

King, D., Walsh, P., and Ciuffreda, F., 1994. Airborne Digital Frame Camera for Elevation Determination. PE&RS 60(11): 1321-1326.

Lichti, D.D. and M. A. Chapman, 1997. Constrained FEM Self Calibration, PE&RS, 63(9): 1111-1119.

Mills, J.P., I. Newton, and R.W. Graham, 1996. Aerial Photography for Survey Purposes with a High Resolution, Small Format, Digital Camera Photogrammetric Record 15 (88): 575-587, October, 1996.

Mostafa, M.M.R., 2003. Design and Performance of the DSS. Proceedings of the 49th Photogrammetric Week, Stuttgart, Germany, September 1-5, 2003.

Mostafa, M.M.R. and K.P. Schwarz, 2001. Digital image georeferencing from a multiple camera system by GPS/INS. ISPRS Journal of Photogrammetry & Remote Sensing 56 (2001): 1-12.

Mostafa, M.M.R. and K.P. Schwarz, 2000. A Multi-Sensor System for Airborne Image Capture and Georeferencing. PE&RS, 66 (12): 1417-1424.

Mostafa, M.M.R., K.P. Schwarz, and P. Gong, 1997. A Fully Digital System for Airborne Mapping, KIS97 Proceedings, Banff, Canada, June 3-6, pp. 463-471.

Schwarz, K.P., M.A. Chapman, M.E. Cannon and P. Gong, 1993. An Integrated INS/GPS Approach to The Georeferencing of Remotely Sensed Data, PE&RS, 59(11): 1167-1674.

Schwarz, K. P., 1995. Integrated Airborne Navigation Systems for Photogrammetry. Proceedings of Photogrammetric Week '95, Eds. D. Fritsch/D. Hobbie, Wichmann, Heidelberg, pp. 139-153.

Škaloud, J., 1999. Problems in Direct-Georeferencing by INS/DGPS in the Airborne Environment. ISPRS Commission III, WG III/1 Barcelona, Spain, November 25-26.

Snay, R.A., 2000. The National and Cooperative CORS Systems in 2000 and Beyond, Proceedings of ION GPS 2000, 19-22 September 2000, Salt Lake City, UT, pp. 55-58.

Tachibana, K., T. Sasagawa, M.M.R. Mostafa, Y. Tanahashi, 2004. Practical Accuracy Analysis of the DSS Test Flights in Japan. CD-Rom Proceedings of the ASPRS Annual Meeting, Denver Colorado, USA, May 23-28.

Toth, C. and D.A. Grejner-Brzezinska, 1998. Performance Analysis of The Airborne Integrated Mapping System (AIMSTM), International Archives of Photogrammetry and Remote Sensing, 32 (2):320-326.